



Mapping of Geological Structural Features in Lolgorien, Narok County, Kenya: Using Hillshade Analysis

Sammy O. Ombiro^{1*}, Akinade S. Olatunji², Eliud M. Mathu³ and Taiwo R. Ajayi²

¹Pan African University, Life and Earth Sciences Institute, University of Ibadan, Ibadan, Nigeria.

²Department of Geology, University of Ibadan, Ibadan, Nigeria.

³Department Geology and Meteorology, South Eastern Kenya University, Kitui, Kenya.

*Corresponding author, e-mail: sombiro@jkuat.ac.ke

Co-authors' e-mails: akinadeshadrach@yahoo.com; emathu@seku.ac.ke; traajai66@gmail.com

Received 16 Jan 2021, Revised 9 Mar 2021, Accepted 21 Apr 2021, Published May 2021

DOI: <https://dx.doi.org/10.4314/tjs.v47i2.4>

Abstract

Despite Lolgorien being one of the most active gold mining areas in Kenya, it is one of the most geologically understudied areas. To the best knowledge of the authors, Lolgorien geological map was last updated in the 1940s. Current technologies such as remote sensing allow new structural features such as faults to be easily identified. In this regard, this study employed remote sensed data to map structural features found in and around Lolgorien Subcounty, Narok, Kenya. This was done to identify any new structural features that might have been missed in the past. Shuttle Radar 152 Topography Mission Digital Elevation Model (SRTM-DEM) image was downloaded and analysed using hillshade technique. From this analysis, the research identified new structural features which were not included in the current geological map but exist on the ground. One such structural feature (fault) is located approximately at 9866237, 703601 (Universal Transverse Mercator, UTM coordinates) and trends in NW–SE direction. The study also found that most of the lineaments are concentrated in the southern part of Lolgorien area and around or at areas dominated by the banded iron formations. Petrographic analysis of the few samples collected from the area showed presence of gold, pyrite and chalcocopyrite mineralisation.

Keywords: SRTM-DEM, lineaments, geological structures, hillshade analysis, Lolgorien area

Introduction

Even though identification of lineaments has successfully been done mainly via fieldwork in the past, the exercise is extremely difficult, and at times costly, especially if aerial photography is involved (Radaideh et al. 2016, Shake and McHone 1987). As a result, chances of missing a structural feature during the exercise are relatively high when compared to when remote sensing and Geographic Information System (GIS) techniques are employed. In fact, mapping of lineament using remote sensing is an important aspect of the current structural and neotectonic studies. This

is because lineament mapping as mentioned by Shake and McHone (1987), Gabrielsen et al. (2002), Kadarusman et al. (2004), Ramli et al. (2010), Masoud and Koike (2011a), Masoud and Koike (2011b) and Radaideh et al. (2016) give important clues about late Quaternary tectonic deformation.

Extraction of lineament from remote sensed data can be achieved through automatic lineament extraction via appropriate software applications such as PCI Geomatica or via manual visualisation and extraction. Muhammad and Awdal (2012) noted that of these two lineament extraction techniques,

automatic technique is preferred by many researchers for its speed of extraction and efficiency when compared to the manual process. However, the accuracy and reliability of automatic extraction of lineament depends on several factors. For instance, automatic lineament extraction cannot distinguish geological lineaments from non-geological ones such as railway lines, power lines, fences amongst others (Muhammad and Awdal 2012). As a result, the resulting lineament map may contain additional features besides the already mapped geological features (Leech et al. 2003, Radaideh et al. 2016).

Before extraction of lineaments, raw images from which the lineaments are to be extracted must be processed. Processing of the images highlight these features making them distinguishable from other features. One technique used in highlighting these features is called hillshade analysis. According to Jordan and Schott (2005), Arrowsmith and Zielke (2009), Masoud and Koike (2011b), Masoud and Koike (2011a), and Langridge et al. (2014), hillshade technique is widely employed in identification of lineaments in regions which are tectonically active because of high accuracy involved. This means that the technique is mainly used to accurately map topographical features found on the Earth's surface. As explained by Radaideh et al. (2016), hillshading technique is based on simulation of relief features (especially linear relief features) by an artificial light illuminating the relief feature from a point source with a specific azimuth and altitude (elevation). Depending on the illumination azimuth and tilt chosen, the topographical features being investigated can either be highlighted or obscured (Radaideh et al. 2016). It is however, important to note that features that are parallel to the beam of light being illuminated are not easy to identify when compared to features that are oriented perpendicularly to the light being illuminated (Cooper 2003, Abdullah et al. 2010, Muhammad and Awdal 2012). It is, therefore, important that this biasness is removed during analysis. This is often achieved by applying

different azimuth values of sun rays to the hillshaded image.

A number of remote sensed data can be used to extract lineaments. Some of the remote sensed data are Land Remote Sensing Satellite (Landsat) data, Advanced Spaceborne Thermal Emission and Reflection Radiometer (ASTER) data, Shuttle Radar Topography Mission (SRTM) and Cartosat (Cartography and Satellite) data. When Landsat data were compared to ASTER data, Hung et al. (2005) and Hubbard and Thompson (2012) found that ASTER data are more accurate in identification of lineaments since they produce less noise than equivalent Landsat bands. Because of this, ASTER short-wave infrared (SWIR) bands (especially the 10-m resolution) are widely used in mapping linear trending spectral-tonal contrast associated with epithermal phyllic alteration instead of equivalent Landsat bands (Mars and Rowan 2007, Hubbard and Thompson 2012). When ASTER data were compared to SRTM data, Rajasekhar et al. (2018) found that SRTM data identify more lineaments than ASTER data and are more accurate.

It is important to note that structural features play important roles in mineralisation. Because of this, their mapping may help geoscientists in locating areas of possible mineralisation. This is because they form potential pathways through which mineralised fluids may use to migrate and thus mineralising the adjacent wall rock or forming mineralised veins (Suh 2009, Fon et al. 2012, Hallarou et al. 2020). These minerals may be identified through petrographic analysis, geochemical analysis or naked eye in some instances.

Despite the important role that Lolgorien area plays in the production of gold, it remains one of the most geologically understudied areas in Kenya. To the best knowledge of the authors, the last geological study carried out on the area, other than the ones being carried out by the mining companies, was published by Ichang'i and MacLean (1991). Furthermore, their findings were not specific to Lolgorien but covered the entire Migori Greenstone Belt

leaving only one study which was carried out in the 1940s by Shackleton (1946) on behalf of the Geological Survey of Kenya. In this context, an attempt was made to bridge this gap by employing remote sensed data to map structural features (lineaments) controlling gold mineralisation in Lolgorien area. The newly identified structural features (lineaments) were included in the current geological map of Lolgorien and a new updated geological map produced.

Geological Setting of the Study Area

Study area location

The study area which is part of the large East African Rift Valley is located in Lolgorien Sub-County situated in Narok County in the western part of Kenya (Figure 1). The geographic coordinates of Lolgorien are 1° 14' 0" S, 34° 48' 0" E.

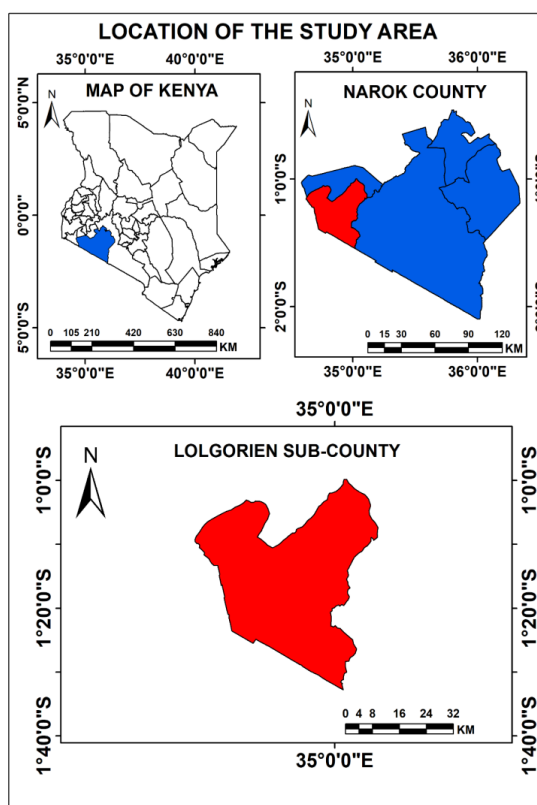


Figure 1: Location of the study area.

Geological setting

Regional geology

Lolgorien gold fields are located along the Nyanzian greenstone belt which is an extension of Archean Greenstone Belt located in the neighbouring Tanzania, Congo and Uganda (Shackleton 1946, Ichang'i and MacLean 1991, Henckel et al. 2016). This belt is generally

composed of continuous volcano-sedimentary successions and granitic intrusions (Henckel et al. 2016). It is divided into the southern and northern terranes by the Winam gulf (branch of the Great East African Rift System) (Shackleton 1946, Ichang'i and MacLean 1991). Granites and greenstones are generally exposed in the southern western part of the rift

around the Rangwa carbonatite complex and in the northeast indicating that the belt is generally continuous along the rift. In the northern terrane, the greenstones which tend to trend in the east-west direction are dominated by sequences of volcanic rocks (Shackleton 1946). They also overly turbiditic sedimentary rocks considered to be part of the Kavirondian group. The greenstones in the southern terrane which host the Lolgorien gold fields generally trend to the northwest direction (Ichang'i and MacLean 1991). The greenstones mainly consist of felsic volcanics with generally low amounts of mafic lavas, polymictic conglomerates, and turbiditic sediments. The belt is also associated with banded iron formations within the greenstone ridges (Murray-Hughes 2007). These greenstones are generally overlain to the eastern side by Proterozoic Kisii volcanics, to the southeast by Tertiary Rift volcanics and to the northwest also by Tertiary Rift volcanics (Murray-Hughes 2007).

The volcano-sedimentary rocks which form most part of the Nyanza greenstone belt are generally vertical or dip steeply (Henckel et al. 2016). Some of these rocks are tightly to isoclinally folded (Shackleton 1946, Ichang'i and MacLean 1991, Ichang'i 1993). Even though some of the formations are overturned, primary geological features such as boulders, graded bedding planes, flow tops and pillows are preserved (Shackleton 1946, Ichang'i and MacLean 1991, Murray-Hughes 2007). Metamorphism in the southern and the northern terranes has resulted into greenschist facies mineral assemblages "that grade to amphibolite facies at the margins of major granitic intrusions" (Ichang'i and MacLean 1991).

The Kenyan Geology is generally grouped into five geological successions, namely: Archean; Palaeozoic and Mesozoic sediments; Proterozoic (consisting of Bukoban and Mozambique belt); Tertiary and Quaternary sediments; Tertiary and Quaternary volcanics (Akech et al. 2013). The Archean consists of

the Kavirondian and Nyanzian systems and form part of the Tanzanian Craton. They are the oldest rocks in Kenya (Akech et al. 2013). The Nyanzian system is generally composed of pyroclastic and lava with banded iron formations and minor sediments. It also consists of basalts, cherts, ironstones, rhyolites, andesites and shales (Akech et al. 2013). The Kavirondian system consists of sandstones, conglomerates, greywackes and grits. Both of these systems are folded isoclinally and their axes tend to trend towards the east-westerly direction. Even though the Kavirondian system is slightly younger than the Nyanzian system, they fold in a similar orientation. Generally, the two systems have been intruded by numerous batholiths and granitic intrusions. The Kavirondian and Nyanzian systems are an extension of the Tanzanian craton where mining of base and precious metals mineralisation takes place. Metallic minerals such as silver, gold and copper have been found (Akech et al. 2013).

Local Geology

The geological units found in Lolgorien may be grouped into the following successions: Nyanzian units, Kavirondian units, Bukoban units and Miocene and Pleistocene. Nyanzian units as already discussed consist of conglomerates, shale, greywacke, banded iron formations, pillow lavas and basalt, granites, tuffaceous and slaty rocks. Kavirondian units consist of boulder conglomerates, shales and sandstones. Bukoban units mainly consist of porphyritic and non-porphyritic basalts and are found on the northern part of Lolgorien as shown in geological map (Figure 2). Miocene mainly consist of the phonolites, and are generally located on the eastern side of Lolgorien. The gravels form part of the Pleistocene rock units and are generally found throughout Lolgorien area. The Nyanzian units form the bulk of rocks found in Lolgorien as shown in Figure 2.

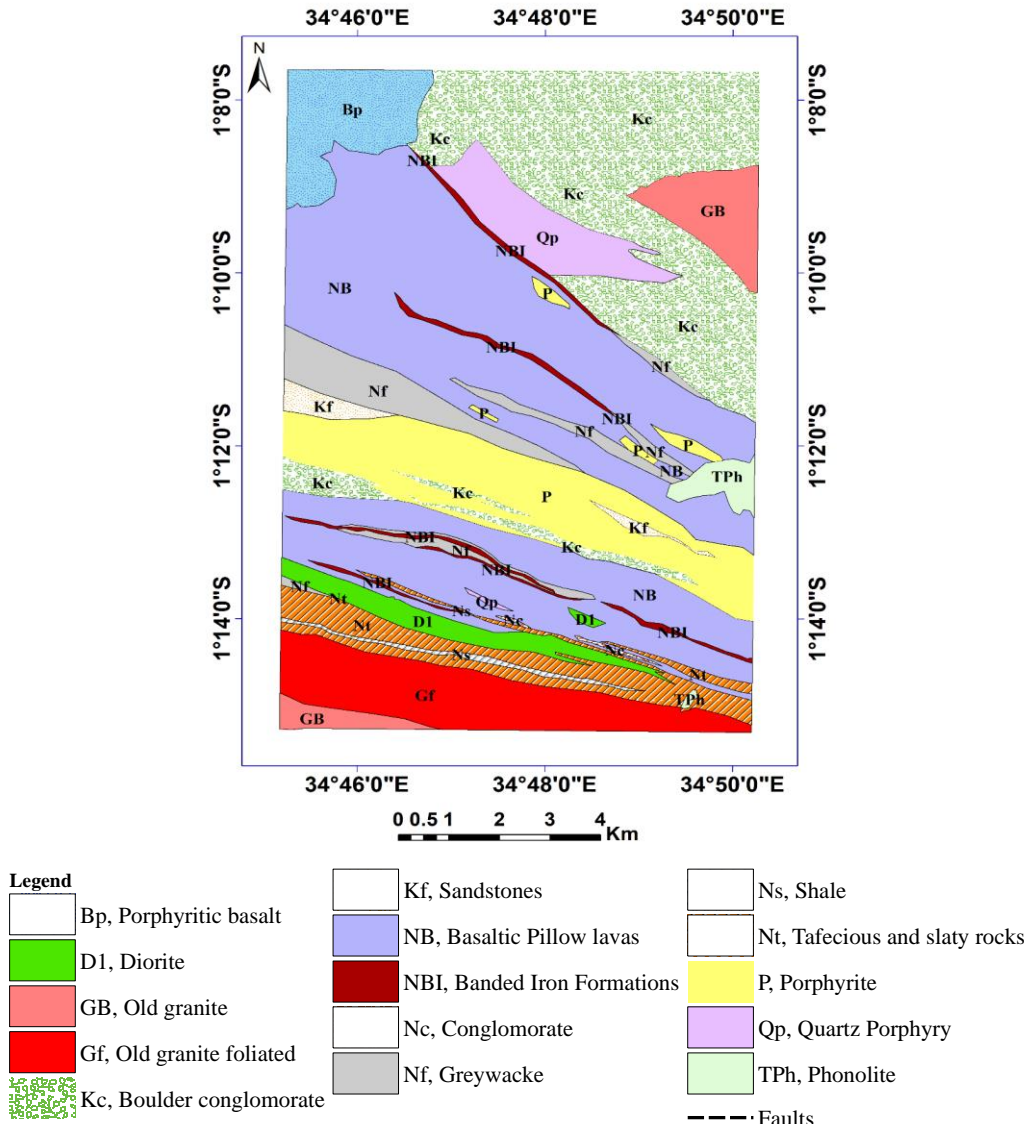


Figure 2: Geological map of Lolgorien (modified after Shackleton 1946).

Materials and Methods

Data acquisition

The main data used in the extraction of the lineament for Lolgorien are Shuttle Radar Topography Mission (SRTM) Digital Elevation Model (DEM) data with resolution of 30 m. SRTM DEM data were chosen because they are more accurate in the identification of

lineaments when compared to Landsat data and ASTER data. The study area was covered by one SRTM DEM image. This SRTM DEM image had an identification of number (ID) of SRTM1S02E034V3 and a resolution of 1-ARC second (30 m) (USGS 2014). The general coordinate of the image was -2, 34 (S-2°, E34). The data were acquired on 27th August, 2020

from United States Geological Survey (USGS) database. From the image, hill-shaded images were developed and for each image, lineaments were subsequently extracted.

Data processing

In order to identify the lineaments, hillshade images were derived from the SRTM DEM image using ArcGIS 3D Analyst tools. This was done by applying 3 azimuth values to the SRTM DEM image, namely: 315°, 200°, and 100°. The results are shown in Figure 4. From the figure it is observed that some linear features were not clearly identified in one azimuth angle of the light source but identified in another azimuth angle. After hillshade processing of the images, the lineaments were extracted using manual technique instead of automatic extraction using software applications such as PCI Geomatica. Manual extraction was preferred over automatic extraction because it was able to discriminate non-geological features such as roads, railways and buildings from the geological lineaments.

The results of lineament extraction are shown in Figures 3 and 4.

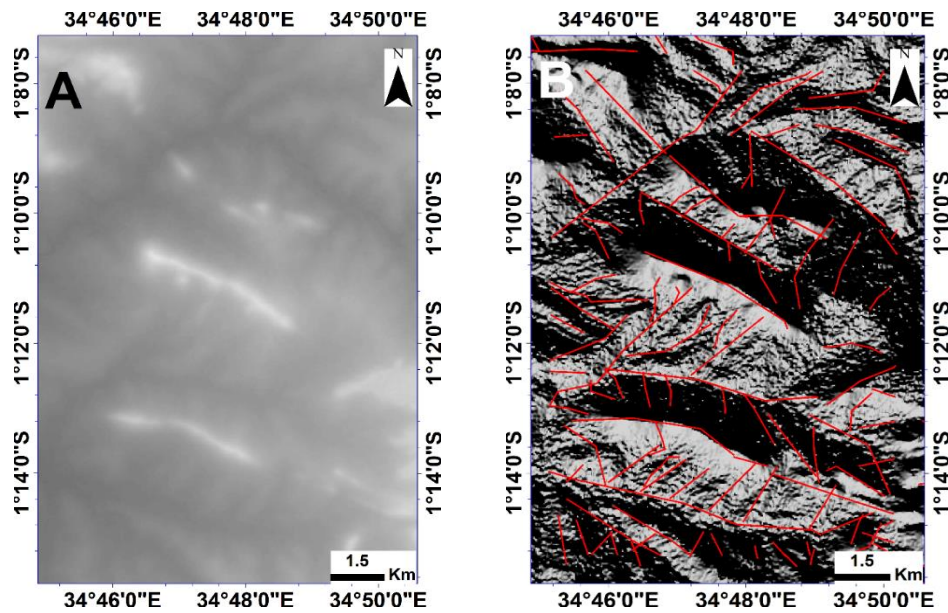
Ground truthing

Ground truthing was also conducted to ascertain the remote sensing findings. The fieldwork was conducted at several locations. The interesting sites, deformations and rock units spotted in these locations were located using Garmin Global Positioning System (GPS). As mentioned earlier, this exercise was carried out to validate whether or not, the lineaments identified were existing. The general orientations of the validated structural features were measured using a geological compass. These orientations are displayed in rose diagrams.

Results and Analysis

Lineament extraction results

The results of lineament extraction are shown in Figure 3.



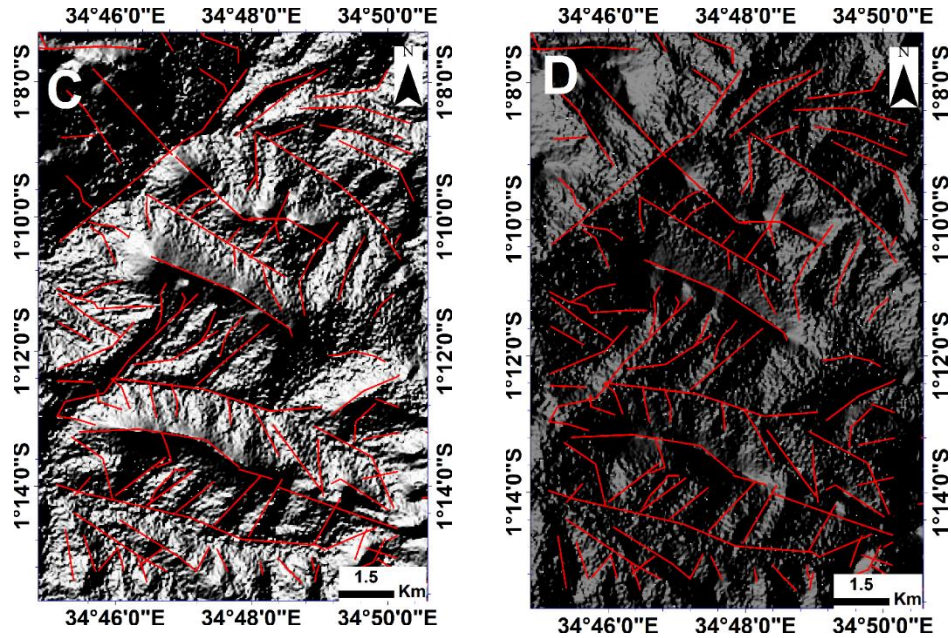


Figure 3: The various hillshade images. A) Unprocessed SRTM-DEM image downloaded from USGS database. B) Hillshade processed image at azimuth of 200° and dip of 50° . C) Hillshade processed image at azimuth of 315° and dip of 45° . D) Hillshade processed image at azimuth of 100° and dip of 60° .

The results showing the extracted lineaments, lineament density map and rose diagrams are shown in Figure 4.

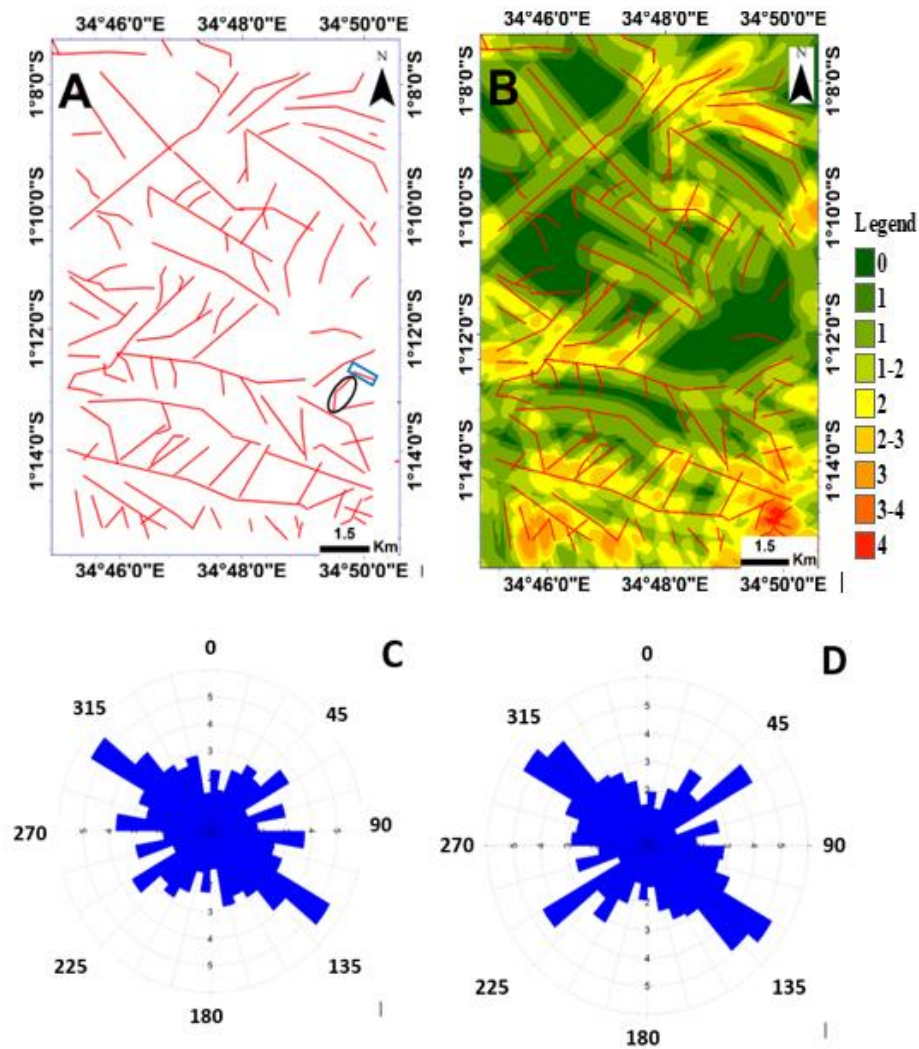


Figure 4: A) Lineaments extracted from the hillshade images (enclosed in a blue rectangular box is the newly identified lineament and enclosed in black oval shape is an existing fault). More details of the features are shown in Figure 5. B) Lineament density map. The legend shows the number of lineaments found in each coloured zone. C) Lineament frequency rose diagram. D) Lineament length rose diagram.

Fieldwork and laboratory results

Figure 5 shows photos of some of the faults identified during the fieldwork.



Figure 5: A) A newly identified fault line by the remote sensed image and is not shown in the current geological map. (B) An existing fault line accurately identified and located by the remote sensed image. These lineaments are accurately shown in Figure 4 and updated in geological map shown in Figure 6. The general location where these lineaments are found is 9866237, 703601 (UTM) coordinates which coincide geographically with the location shown on the lineament map (Figure 4A). However, due to thick vegetation and difficult terrain, it was impossible to develop extended photographic illustration of lineaments.

Figure 6 shows the updated geological map of Lolgorien based on the identified structural features.

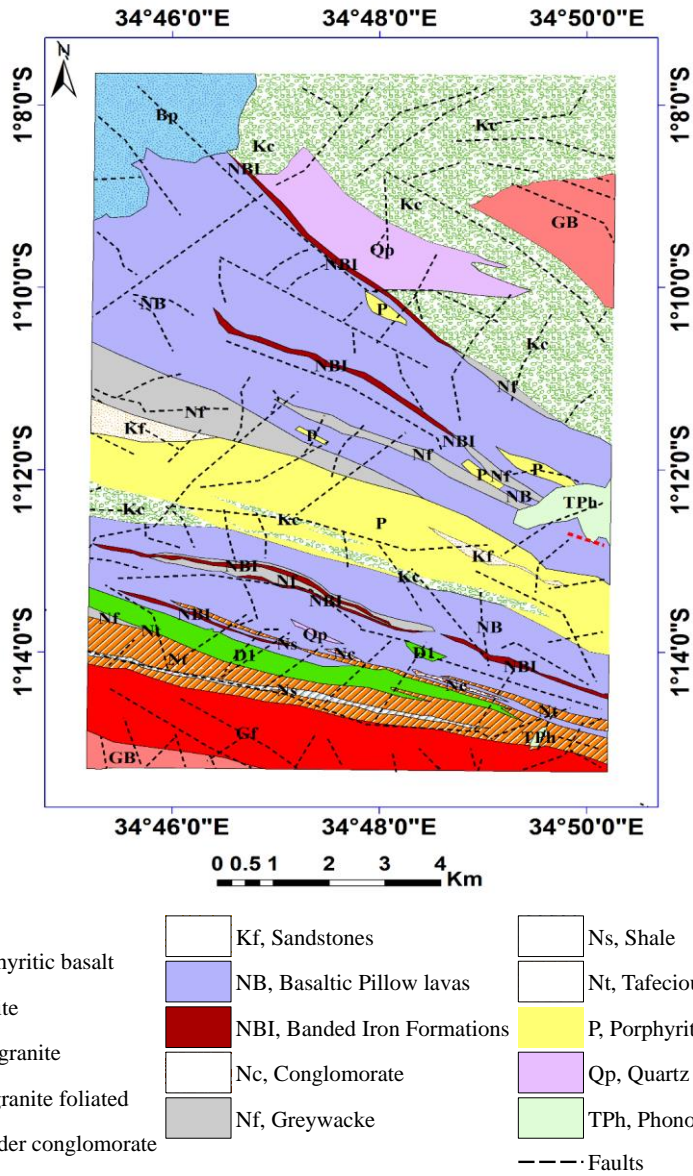


Figure 6: Updated geological map of Lolgorien. The red lineament (red dotted line) is the newly identified fault line.

Figure 7 is the current geological map of Lolgorien area.

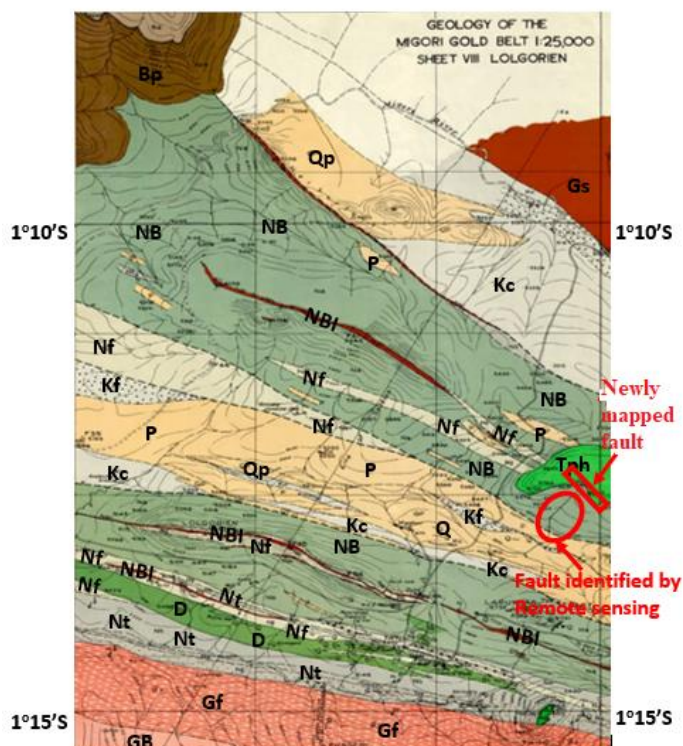


Figure 7: The current geological map of Lolgorien (modified after Shackleton 1946). Bp = Porphyritic basalt, D = Diorite, GB = Old granite, Kc = Boulder conglomerate, Kf = Sandstones, NBI = Banded Iron Formations, Nc = Conglomerate, Nf = Greywacke, Ns = Shale, Nt = Slaty rocks, Qp = Quartz porphyry, Tph = Phonolite.

Figure 8 shows a hand specimen of a fractured banded iron formation rock (A) and a quartz vein dipping into ground (A). It is,

however, important to note these images were not taken from the same place. That is, A is not part of B.

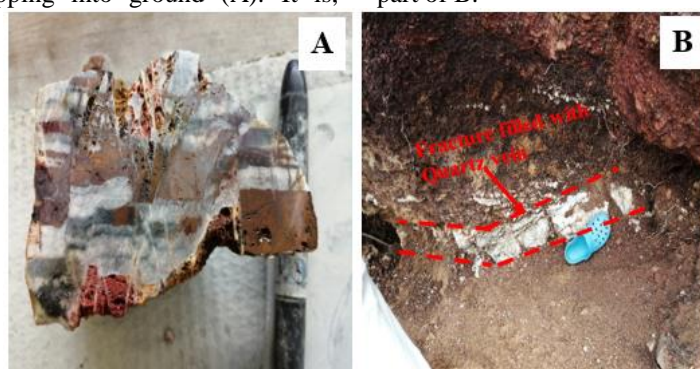


Figure 8: A) A fractured banded iron formation rock. The fractures are filled with quartz veins. B): A quartz vein dipping into ground.

Figure 9 shows photomicrographs of the fractured banded iron formation shown in XPL X100

Figure 8A.

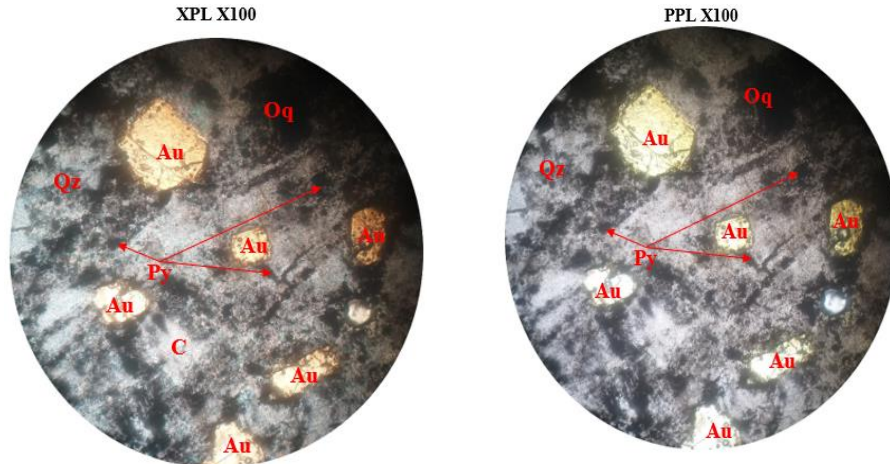


Figure 9: Photomicrograph of banded iron formation showing opaque (Oq) minerals such as magnetite and hematite, quartz (Qz), gold (Au) and pyrite (Py). The first image is a XPL (crossed polarised light) image, while the second image is the PPL (plane-polarised light) image. Minerals behave differently under different light conditions making them absent (diminish) under one light condition (say under PPL) and present under another (say XPL). Having both XPL and PPL images, therefore, maximises the chance of identification of the mineral crystals forming a rock sample.

Discussion

Several linear structures were identified from the hillshade images and are shown by red lines in Figures 3B, 3C and 3D. These lineament features are valleys, ridges and hill peaks. Hillshade analysis made these features appear more prominent compared to other features found in the surrounding area as shown in Figures 3B, 3C and 3D, and thus enhancing their identification. The geological structures as shown in rose diagrams (Figures 4C and 4D) tend to trend in NW-SE direction which is the same trend as the Lolgorien's geological units (Figures 2, 6 and 7).

The identified lineaments were compared to the fault lines shown in the current Lolgorien geological map (Figure 7), and it was found that all the fault lines shown on the current geological map matched the extracted lineaments. Additionally, new lineaments were identified by the processed remote sensed images that were not shown in the current

geological map of Lolgorien. As shown in Figures 6 and 7, it was observed that while all the lineaments shown in the current geological map were also shown in the lineament map, the vice-versa was not true. That is, not all lineaments shown in lineament map were shown in the geological map. This means that new lineaments were identified in the current study. When ground truthing was carried out in areas that were accessible, it was found that features shown on the remote sensed images matched the ground features. For instance, lineament circled in Figure 4A (lineament map), matched fault line shown in Figure 5B and was correctly mapped as shown in the geological map. Also, lineament marked by rectangular shape on lineament map shown in Figure 4A correctly matched fault line shown 5A. This lineament, however, is not shown in the current geological map. The UTM coordinates of a point on the newly identified fault line is: 9866237, 703601. Fieldwork

confirmed that this fault line tends to trend in NW-SE direction and intersects the fault line shown Figure 5B. When the current geological map and lineament map were further compared, it was found that a number of lineaments shown in the lineament map (Figure 4A and Figure 6) are not shown in the current geological map (Figure 7). It is, however, important to note that because of difficult terrain, thick forest and rainfall during fieldwork exercise, most of these lineaments were unreachable and hence were not mapped by groundwork. It is, therefore, recommended that future studies consider ground truthing of these lineaments.

Figure 4B is a lineament density map showing concentration of lineaments at various parts of the study area. It is observed that most of the lineaments are concentrated in the southern part of Lolgorien area and around or at areas dominated by the banded iron formations (Figures 6 and 7). Lineaments are also concentrated in the central western part of the Lolgorien and in the north eastern part of the study area as shown in Figure 4B. These areas have greater potential for mineralisation when compared to other areas in Lolgorien. This is because structures, especially faults and fractures are potential pathways through which mineralised fluids migrate (Suh 2009, Fon et al. 2012, Hallarou et al. 2020). A ground truthing exercise (fieldwork) showed that these areas, especially the southern part of the Lolgorien hill, are dominated by artisanal mines. Samples collected from the area and were subjected to petrographic analysis showed that these areas were mineralised with gold, pyrite and opaque minerals. The photomicrographic images of samples of banded iron formations collected from the southern part of Lolgorien (area with high lineament density) are shown in Figure 9. The hand samples of these banded iron formations are shown in Figure 8A.

Fieldwork (ground truthing exercise) also proved that indeed the southern part of Lolgorien (the zone with high density of lineaments in accordance with lineament

density map as shown in Figure 4B) is dominated by several fractures some of which are filled by quartz veins such as the ones shown in Figures 8A and B. Figure 8A shows a fractured hand specimen extracted from a BIF outcrop found in the study area. This hand specimen is mineralised as shown in Figure 9 (photomicrographs of thin sections extracted from the specimen). As already discussed, structures (especially faults and fractures) are potential pathways through which mineralised and fluids may migrate. These fluids may undergo silicification process within the fracture resulting into formation of massive quartz veins such as the one shown in Figure 8B.

Because the southern part of the study area which has a high density of lineament is also associated with gold mineralisation, it is concluded that faults and fractures are the major structures controlling gold mineralisation in Lolgorien.

Conclusion

The study employed remote sensed data to map structural features found in and around Lolgorien area (both those controlling gold mineralisation and those that do not control gold mineralisation). The aim of exercise was to update Lolgorien's geological map which to the best knowledge of the authors, was last updated by Shackleton (1946) on behalf of the Geological Survey of Kenya. The remote sensing exercise identified several structural features (lineaments) which are not shown on the current geological map but exist on the ground. One such structural feature is located approximately at 9866237, 703601 (UTM) coordinates and trends NW-SE direction just as geological units found in the area. However, due to the difficult terrain, thick forest and rainfall, most of lineaments identified by analysis of the remote sensed images were unreachable and hence were not mapped by groundwork. It is, therefore, recommended that future studies should consider ground truthing these lineaments.

The study also found that most of the lineaments are concentrated in the southern part of Lolgorien area and around or at areas dominated by the banded iron formations. The southern part of the Lolgorien hill is also dominated by artisanal mines. Few samples collected from the area and subjected to petrographic analysis showed the presence of gold, pyrite and chalcopyrite mineralisation. The central western part of the Lolgorien and the North Eastern part of the study area were not accessible during fieldwork as a result of poor weather, thick vegetation and difficult terrain. As a result, no rock samples were collected. Just as the central part of Lolgorien, these areas have greater potential for mineralisation owing to the large number of lineaments associated with them. It is therefore, recommended that future studies consider rock sampling for mineralogical and structural characterisation.

Acknowledgement

This publication is part of the first author's Ph.D. work and was funded by the African Union through the Pan-African University, Life and Earth Sciences Institute (including Health and Agriculture), University of Ibadan, Nigeria (PAULESI).

References

- Abdullah A, Akhir JM and Abdullah I 2010 Automatic mapping of lineaments using shaded relief images derived from digital elevation model (DEMs) in the Maran-Sungi Lembing area, Malaysia. *Elect. J. Geotech. Eng.* 15(6): 949-958.
- Akech NO, Omuombo CA and Masibo M 2013 Chapter 1- General geology of Kenya. *Dev. Earth Surf. Proc.* 16: 3-10.
- Arrowsmith JR and Zielke O 2009 Tectonic geomorphology of the San Andreas Fault zone from high resolution topography: An example from the Cholame segment. *Geom.* 113(1-2): 70-81.
- Cooper G 2003 Feature detection using sun shading. *Comp. Geosc.* 29(8): 941-948.
- Fon AN, Che VB and Suh CE 2012 Application of electrical resistivity and chargeability data on a GIS platform in delineating auriferous structures in a deeply weathered lateritic terrain, eastern Cameroon. *Int. J. Geos.* 3(05): 960.
- Gabrielsen RH, Braathen A, Dehls J and Roberts D 2002 Tectonic lineaments of Norway. *Nor. Geo. Tid.* 82(3): 153-174.
- Hallarou MM, Konaté M, Olatunji AS, Ahmed Y, Ajayi FF and Abdul RM 2020 Re-Os Ages for the Kourki Porphyry Cu-Mo Deposits, North West Niger (West Africa): Geodynamic Implications. *Euro. J. Env. Earth Sci.* 1(4).
- Henckel J, Poulsen K, Sharp T and Spora P 2016 Lake victoria goldfields. *Epdes.* 39(2): 135-154.
- Hubbard BM and Thompson TJ 2012 Lineament Analysis of Mineral Areas of Interest in Afghanistan: Automatically delineated lineaments using 30-m TM imagery. *U.S. Geol. Surv.* 1048: 28.
- Hung L, Batelaan O, and De Smedt F 2005 Lineament extraction and analysis, comparison of LANDSAT ETM and ASTER imagery. Case study: Suoimuoi tropical karst catchment, Vietnam. Remote sensing for environmental monitoring. *GIS Appl. Geol.* V.
- Ichang'i D 1993 Segment of the nyanza greenstone belt, kenya. *Proc. 5th Conf. Geol. Ken. Geol. Sust. Dev.*
- Ichang'i D and MacLean W 1991 The Archean volcanic facies in the Migori segment, Nyanza greenstone belt, Kenya: stratigraphy, geochemistry and mineralization. *J. Afr. Earth Sci.* 13(3/4): 277-290.
- Jordan G and Schott B 2005 Application of wavelet analysis to the study of spatial pattern of morphotectonic lineaments in digital terrain models. A case study. *Rem. Sens. Env.* 94(1): 31-38.
- Kadarusman A, Miyashita S, Maruyama S, Parkinson CD and Ishikawa A 2004 Petrology, geochemistry and paleogeographic reconstruction of the East

- Sulawesi Ophiolite, Indonesia. *Tect. Phy.* 392(1-4): 55-83.
- Langridge R, Ries W, Farrier T, Barth N, Khajavi N and De Pascale G 2014 Developing sub 5-m LiDAR DEMs for forested sections of the Alpine and Hope faults, South Island, New Zealand: Implications for structural interpretations. *J. Struct. Geol.* 64: 53-66.
- Leech D, Treloar P, Lucas N and Grocott J 2003 Landsat TM analysis of fracture patterns: a case study from the Coastal Cordillera of northern Chile. *Int. J. Rem. Sens.* 24(19): 3709-3726.
- Mars JC and Rowan LC 2007 Mapping phyllic and argillic-altered rocks in southeastern Afghanistan using Advanced Spaceborne Thermal Emission and Reflection Radiometer (ASTER) data. *US Geol. Surv.* 1.
- Masoud AA and Koike K 2011a Auto-detection and integration of tectonically significant lineaments from SRTM DEM and remotely-sensed geophysical data. *ISPRS J. Photo. Rem. Sens.* 66: 818. <https://doi.org/10.1016/j.isprsjprs.2011.08.003>
- Masoud AA and Koike K 2011b Morphotectonics inferred from the analysis of topographic lineaments auto-detected from DEMs: Application and validation for the Sinai Peninsula, Egypt. *Tect. Phy.* 510: 291. <https://doi.org/10.1016/j.tecto.2011.07.010>
- Muhammad M M and Awdal AH 2012 Automatic mapping of lineaments using shaded relief images derived from digital elevation model (DEM) in Erbil-Kurdistan, northeast Iraq. *Adv. Nat. Appl. Sci.* 6(2): 138-147.
- Murray-Hughes R 2007 Geological Survey of Lolgorien Area. Mines and Geology Department, Nairobi.
- Radaideh OM, Grasemann B, Melichar R and Mosar J 2016 Detection and analysis of morphotectonic features utilizing satellite remote sensing and GIS: An example in SW Jordan. *Geom.* 275: 58-79.
- Rajasekhar M, Raju GS, Raju RS, Ramachandra M and Kumar BP 2018 Data on comparative studies of lineaments extraction from ASTER DEM, SRTM, and Cartosat for Jilledubanderu River basin, Anantapur district, AP, India by using remote sensing and GIS. *Data in Brief.* 20: 1676-1682.
- Ramli M, Yusof N, Yusoff M, Juahir H and Shafri H 2010 Lineament mapping and its application in landslide hazard assessment: a review. *Bull. Engin. Geol. Environ.* 69(2): 215-233.
- Shackleton R 1946 Geology of the Migori gold belt. *Geol. Surv. Kenya.* 10.
- Shake SN and McHone JG 1987 Topographic lineaments and their geologic significance in central New England and adjacent New York. *Northeast. Geol.* 9(3): 120-128.
- Suh C 2009 Sulphide microchemistry and hydrothermal fluid evolution in quartz veins, Batouri gold district (southeast Cameroon). *J. Camern. Acad. Sci.* 8(1): 19-30.
- USGS 2014 Full Display of SRTM1S02E034V3. Retrieved from Earth Explorer: <https://earthexplorer.usgs.gov/scene/metadata/full/5e83a3ee1af480c5/SRTM1S02E034V3/>